Exploring the Potential of Aerial and Balloon–Based Observations in the Study of Terrestrial Gamma Ray Flashes

Marek Sommer[1], Tomáš Czakoj[2], Iva Ambrožová[1], Martin Kákona[1,3], Olena Velychko[1,4], and
Ondřej Ploc[1,4]

[1]Nuclear Physics Institute of the Czech Academy of Sciences, Husinec - Řež 130, 250 68 Řež, Czech Republic.
[2]Centrum Výzkumu Řež s.r.o., Husinec - Řež 130, 250 68, Czech Republic
[3]Institute of Experimental Physics of the Slovak Academy of Sciences, Watsonova 47, Košice 040 01, Slovak Republic
[4]Czech Technical University in Prague, Faculty of Nuclear Sciences and Physical Engineering, Břehová 7, 115 19 Prague,
Czech Republic.

Correspondence: Marek Sommer (sommer@ujf.cas.cz)

Abstract. Recently presented measurements of Terrestrial Gamma Ray Flashes (TGF) above thunderstorms onboard aircraft
and weather balloons introduce viable alternatives which could help to overcome limitations inherent in satellite–based ob-
servations, such as significant gamma ray attenuation by the atmosphere. This study explores the potential and implications
of measuring TGFs using aircraft and weather balloons. Utilizing Monte Carlo simulations with the MCNP6 tool, the spatial

5   distributions, fluences, and energy spectra of photons, electrons, and neutrons generated by TGFs are assessed at altitudes of
5 to 50 km. Results indicate that TGFs originating at lower altitudes produce narrower beams compared to those at higher
altitudes, suggesting that weather balloons may be more effective for high–altitude TGFs, such as those associated with sum-
mer thunderstorms or thunderstorms in tropical regions. Whereas staffed aircraft might be more suitable for low altitude TGFs
originating in temperate regions or in winter thunderstorms. Photon and electron energy spectra features, including maximum

10 energy, and the presence of 511 keV photons, can help estimate the radial distance from the TGF axis. Expected photon flu-
ences from TGFs range from 1 to 10,000 cm^{-2}, with electron fluences ranging from 1 to 1,000 cm^{-2}, depending on the TGF's
brightness. Neutron fluences are notably lower, up to 10 cm^{-2}. These findings underscore the potential of aerial and balloon–
based measurements to provide critical insights into TGFs and their detection, addressing the limitations of current satellite
observations.

15 ## 1   Introduction

The phenomenon of Terrestrial Gamma Ray Flashes (TGF) was discovered in 1994 by (Fishman et al., 1994). TGFs are associ-
ated with lightning, during which extremely intense bursts of radiation are emitted withinhundreds of microseconds (Cummer
et al., 2011, 2015; Østgaard et al., 2021; Marisaldi et al., 2019). Thousands of TGFs have been observed and registered on-
board the International Space Station (ISS), satellites, airplanes (Smith et al., 2011; Bowers et al., 2018), weather balloon

20 (Helmerich et al., 2024), and on the ground (so–called downward TGFs) (Tran et al., 2015; Enoto et al., 2017; Wada et al.,
2019). The majority of TGFs have been detected by detectors on satellites, namely the Reuven Ramaty High Energy Solar

Spectroscopic Imager (RHESSI) (Grefenstette et al., 2009), Astrorivelatore Gamma a Immagini Leggero (AGILE) (Marisaldi et al., 2010, 2014; Maiorana et al., 2020), Gamma–ray Burst Monitor (GBM) (Briggs et al., 2010; Roberts et al., 2018), and Atmosphere–Space Interactions Monitor (ASIM) (Neubert et al., 2019).

25   Most of the detected TGFs were registered in low latitudes, mainly due to the low inclination of the satellites. However, it has been observed that there is a lower TGF–to–lightning ratio in latitudes over 30°. (Maiorana et al., 2021) proposed that this dependence is mainly caused by atmospheric absorption of gamma rays due to the elevated tropopause in equatorial regions.

    The number of bremsstrahlung photons generated during TGFs has been extensively discussed, with estimations ranging from 10^{17} up to 10^{20} gamma rays (Dwyer and Smith, 2005; Gjesteland et al., 2015). In (Celestin et al., 2015) the existence of
30   TGFs with lower intensities was proposed. The energy spectrum of gamma rays reaches very high energies, up to tens of MeV (Grefenstette et al., 2009; Marisaldi et al., 2010; Tavani et al., 2011; Marisaldi et al., 2019).

    Despite numerous observations and studies of various TGFs, the mechanisms of TGF origin that would explain the generation of such a large number of high–energy gamma rays are not well understood. Several theories are under research (Dwyer, 2008; Celestin and Pasko, 2011; Petrov, 2021; Zelenyi et al., 2019; Stadnichuk et al., 2021, 2023).

35   Although there has been an increase in downward TGF measurements in recent years, the majority of TGF detections were performed from space. Measurements from Earth's orbit have several disadvantages, such as a low number of registered photons due to the large distance between the source and detector, blurring of the TGF time structure also due to large distances, and the high speed of the satellite prevents them from staying above a thunderstorm for a long period of time. These factors complicate the study of TGF energy spectra and time structure, and observations of TGFs in mid–latitudes.

40   As recognized by (Lyu et al., 2023), significant new discoveries may arise from joint measurements of a single event from both below and above, involving on–ground and orbital observations. Satellites, due to their high velocities, are limited in their ability to focus on a single thunderstorm over an extended period. However, airplanes or weather balloons offer a viable alternative, as they can be strategically positioned in or above thunderstorms to monitor TGF activity, potentially yielding insights that satellites cannot. Airplanes generally avoid thunderstorms to protect passengers and avoid damage. Furthermore,
45 there are radiation risks associated with flying over TGFs (Dwyer et al., 2010; Tavani et al., 2013; Pallu et al., 2021; Maia et al., 2024). Nevertheless, overcoming these challenges offer a possibility to significantly extend the TGF observations as was demonstrated in (Bowers et al., 2018; Smith et al., 2011; Ostgaard et al., 2023). The measurements on uncrewed weather balloons is nearly risk free and recently it has also been demonstrated that they are feasible for investigation of TGFs (Helmerich et al., 2024).

50   The recent ALOFT campaign, which used an ER-2 aircraft to fly above thunderstorms in the vicinity of the Gulf of Mexico, is noteworthy. The aircraft flew at an altitude of 20 km and gathered 60 hours of flight time, registering 130 TGFs (Ostgaard et al., 2023). These observations suggest that the number of TGF–producing lightning events is much higher than previously believed based on satellite data alone. It indicates that performing measurements in the vicinity of thunderstorms (especially above thunderstorms) might yield new high–quality TGF data. Measurements above the thunderstorms could be conducted in
55 the future by regular jet airplanes or weather balloons.

In this paper, we investigate the detectability of TGFs at altitudes reachable by airplanes and weather balloons (5–35 km). We calculate the fluences and energy spectra of various radiation types as a function of TGF altitude of origin and radial distance from the axis of the beam. The calculations are performed by Monte Carlo software MCNP–6 (Goorley et al., 2013). The results provide estimations of the fluences obtainable by measurements onboard aircraft or weather balloons including the energy spectra. The energy spectra of particles are shown in relation to vertical and radial distance from TGF origin. The results are discussed in regards to the technical constraints for detectors to detect TGF and the implementability of such measurements onboard aircraft or weather balloons. Similar efforts have been made by (Hansen et al., 2013; Ursi et al., 2022), who focused solely on gamma–ray particles and the estimation of generated photons. This work extends the analysis to other particle types, such as electrons and neutrons and also includes the energy spectra of the particles.

2 Materials and Methods

2.1 TGF Monte Carlo simulations

The simulations were performed using the general–purpose 3D Monte Carlo particle transport simulation tool, MCNP6 (Goorley et al., 2013). To estimate the fluences and spatial distributions of particles generated by TGFs at various altitudes, the transport of accelerated particles through the atmosphere was simulated. The calculations were conducted using the NRLMSISE-00 atmosphere model, which accounts for variations in air composition and density as a function of altitude. The Monte Carlo model of the atmosphere was constructed up to an altitude of 50 km in discrete steps of 100 m, with different densities and compositions. The air nuclides considered in the model were ^{14}N, ^{16}O, and ^{40}Ar. Water content in the atmosphere was not considered in the calculations. The primary particles used as input in the model were electrons with an energy spectrum calculated by Dwyer (2011). This spectrum was derived based on the relativistic runaway electron avalanches theory. The point source emitted the accelerated electrons upward in a vertical direction. The source altitudes of 5, 10, and 15 km were used in simulations. These altitudes should represent the approximate altitudes of the high clouds in polar, temperate, and tropical regions respectively (Oceanic and Administration, 2023). The number of primary particles in these calculations was $2.78*10^9$, $2.64*10^9$, and $2.63*10^9$, respectively. The particles produced from the interactions of primary electrons were scored by various tallies, including a cylindrical mesh tally for evaluating fluences and standard tallies for scoring the energy spectra of ionizing radiation particles. The number of inputted electrons with energies >1 MeV in the simulations varied. The results of fluences scored by cylindrical mesh tallies were normalized to 10^{18} particles of primary electrons (>1 MeV) to estimate the flux for a TGF. The results show fluences and spatial distribution of electrons, photons, and neutrons. The Earth's magnetic fields were not considered in the simulations.

The energy spectra of particles were tallied during their passage through surfaces at different altitudes. The simulated cylindrical volume was divided into smaller cylinders to allow the segmentation of the tally surfaces (with a segmentation step of 1 km in cylinder radius).

The physics settings in calculation were set that production of bremsstrahlung and photonuclear reactions was on. The energy cut–offs for electrons, photons and neutrons were 10 keV, 10 keV, and 10^{-6} keV respectively. The cylindrical mesh tallies had

radii of 40 km with steps of 40 m, altitude from 50 m up to 50 km with steps of 50 m and one angle from 0° up to 360°. The
90   Earth's magnetic fields were not considered in the simulations.

3   Results

3.1   Photon fluence

The spatial distribution of photon fluences is depicted in Fig. 1. Fig. 1 shows fluences for three different altitudes of TGF
origin: 5 km, 10 km, and 15 km. It can be observed that the photon beam has the shape of a cone. The opening angle of the
95   cones increases with the altitude of the TGF origin. When the altitude of the TGF origin is at 5 km, the fluence of at least
10 cm^{-2} extends up to an altitude of nearly 25 km, with a radial spread of up to 6 km from the origin. For a TGF origin
at 10 km, the irradiated cone rapidly elongates and widens – the 10 cm^{-2} threshold region reaches up to an altitude above
50 km (beyond the simulation boundaries) with a radial spread of almost 20 km at its maximum. In the case of a TGF at an
altitude of 15 km, the region with fluence higher than 10 cm^{-2} stretches beyond the simulation boundaries of 50 km in altitude
100 and a radial distance of over 40 km. At an altitude of 20–35 km (reachable by weather balloons), the radial distance of the
detectability region ranges from 20 km up to 35 km. The influence of TGF altitude on the beam opening angle has implications
to the Monte Carlo simulations previouslz preformed as the opening angle of the beam is typically a given parameter (Hansen
et al., 2013; Marisaldi et al., 2019; Ursi et al., 2022). Another implication is that TGFs originating at higher altitudes can be
measured at larger distances. Therefore, platforms such as weather balloons which can climb up to 35 km are more suitable
105 for high altitude TGFs. It can be seen that the TGF altitude is an crucial parameter influencing the irradiated volume by the
bremsstrahlung photons and the beam shape. This has a significant consequences for all measurements performed above the
thunderstorms as it defines the detectability regions together with the brightness of TGF and its energy spectrum. Another
consequence of this finding is that the Monte Carlo simulations performed

The photon energy spectra were recovered for various radial distances from the TGF origin. Fig. 2 shows the energy spectra
110 of photons at three different altitudes: 25, 20, and 15 km, as a function of radial distance from the axis of the TGF originating at
an altitude of 10 km. It can be seen that for various radial distances, the ratio between low–energy (< 100 KeV) and high–energy
(> 1 MeV) components changes. High–energy component is more substantial near the axis of the TGF. It can also be observed
that the maximum energy of photons decreases as the radial distance increases. Hence, there is a softening of the gamma–ray
energy spectra at the edges of the irradiated cones. This effect has been observed by (?). This effect is especially pronounced at
115 higher altitudes. Notably, immediately above the TGF, a distinct sharp edge appears in the energy spectrum (approximately at
50 MeV), which corresponds to the maximum energy of primary electrons. However, at a lower radial distance from the center
of the TGF, this sharp edge diminishes and transitions into a continuum. The visible peak between 497–599 keV is caused by
511 keV photons from the annihilation of positrons. The positrons are created mainly by the pair production of high–energy
photons. The 511 keV peak is more pronounced at higher altitudes and at distances closer to the axis of the TGF. These features
120 of the photon energy spectrum (softening of the beam at the edges, and the presence of a 511 keV peak) could be used for
estimating the radial distance to the TGF axis.
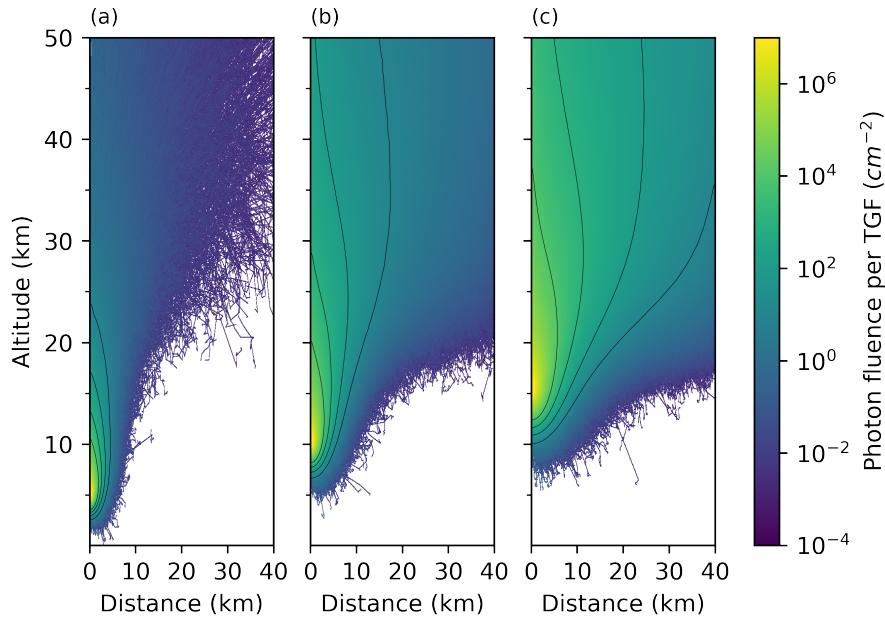
Figure 1. Fluence of photons caused by a TGF at an altitude of A) 5 km, B) 10 km, C) 15 km. The depicted isobars show photon fluences of $10^1, 10^2, 10^3, 10^4$ cm^{-2}.
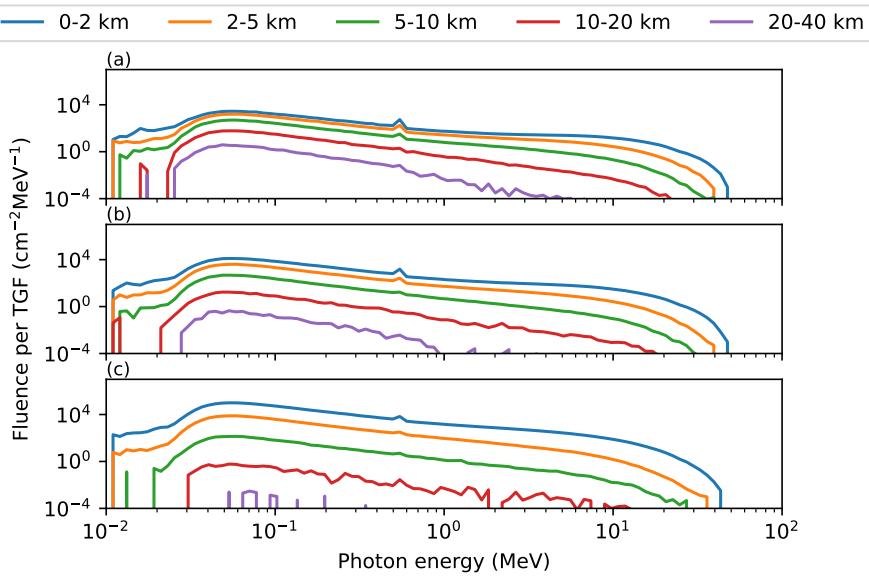
Figure 2. Energy spectra of photons caused by a TGF at different radial distances from the TGF origin. The altitude of the TGF origin is 10 km, and the energy spectra are recorded at altitudes of A) 25 km, B) 20 km, C) 15 km.
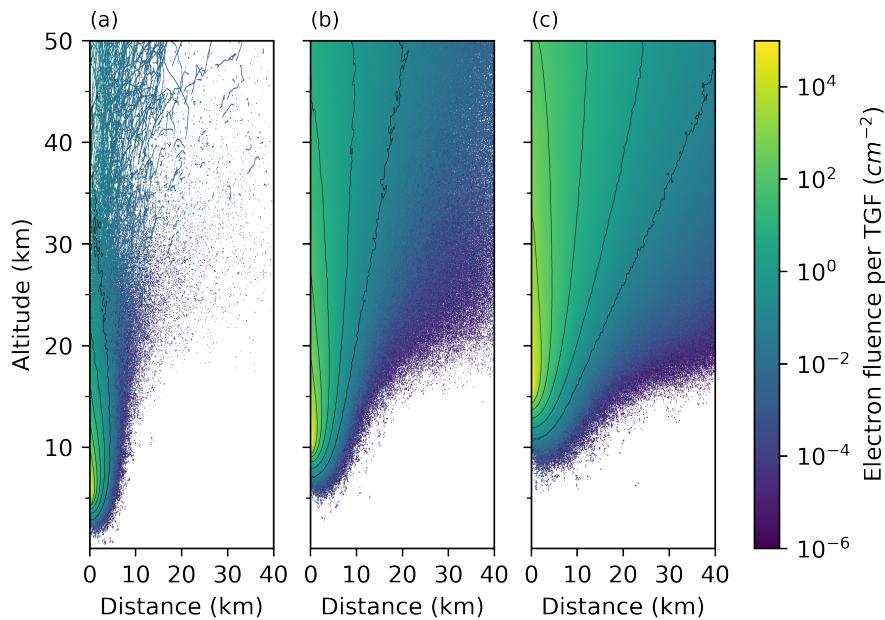
Figure 3. Fluence of electrons caused by a TGF at an altitude of A) 5 km, B) 10 km, C) 15 km. The depicted isobars show electron fluences of 10^{-1}, 10^{0}, 10^{1}, 10^{2}, 10^{3} cm^{-2}.

3.2 Electron fluence

The spatial distribution of electron fluences is depicted in Fig. 3. Fig. 3 shows fluences for three different altitudes of TGF origin: 5 km, 10 km, and 15 km. The spatial distribution of electrons is similar to the photon distribution, as most of the electrons are created by interactions of gamma rays with atoms in the atmosphere. Nevertheless, electron fluences have some specific characteristics. It can be seen that the largest fluences are located in smaller and narrower cones than those observed for gamma rays. Another characteristic of the electron fluence distribution is the presence of long tracks of individual high–energy electrons that are created by interactions of gamma rays with the atmosphere. These tracks are visible in the high–altitude section (a), showing TGFs with an origin at 5 km. Such electrons have large energies and can travel significant distances in the air.

The energy spectra of electrons caused by a TGF at different radial distances are shown in Fig. 4. Similar to photons, the high–energy part of the electron energy spectrum is focused mainly around the center of the TGF, whereas on the edges of the cone, the energy spectrum softens. Although the overall number of electrons decreases as they move to higher altitudes, the shapes of the energy spectra do not undergo significant changes and remain relatively stable.
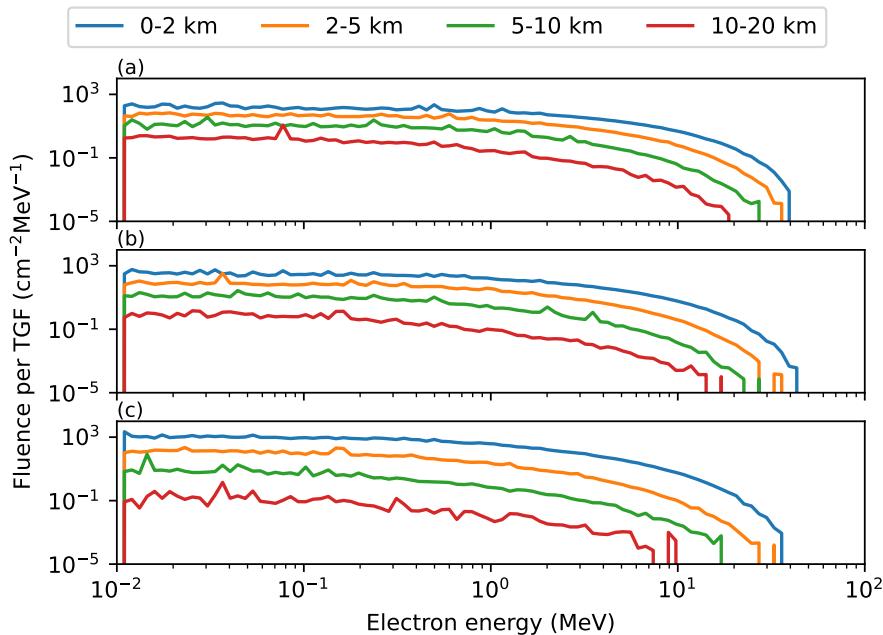
Figure 4. Energy spectra of electrons caused by a TGF for different radial distances from the TGF origin. The altitude of the TGF origin is 15 km, and energy spectra are recovered from altitudes of A) 30 km, B) 25 km, C) 20 km.

3.3 Neutron fluence

The spatial distribution of neutron fluences is depicted in Fig. 5. Fig. 5 shows fluences for three different altitudes of TGF origin – 5 km, 10 km, and 15 km. Neutrons are generated by photonuclear reactions of high–energy gamma rays with atoms of the atmosphere. These reactions have low cross–sections; therefore, the resulting neutron fluences are lower than those of gamma rays or electrons. Moreover, the regions with sufficient neutron fluences (at least $1 \ \mathrm{cm}^{-2}$) are relatively small compared to those of electrons and photons. For these reasons, photoneutrons are likely to be missed or their contribution in the detector would be insignificant. Nevertheless, the absence of detected neutrons can still be valuable for estimating the minimal distance between the radiation source and the detector.

The energy spectra for two different radii are shown in Fig. 6. It can be seen that neutron energy spectra are very insensitive to the radial distance from the axis of the TGF. The most significant portion of neutrons are thermal neutrons. The neutron energy spectra are not significantly influenced by the altitude at which they were tallied. However, the low statistics cause the energy spectra to exhibit noise.
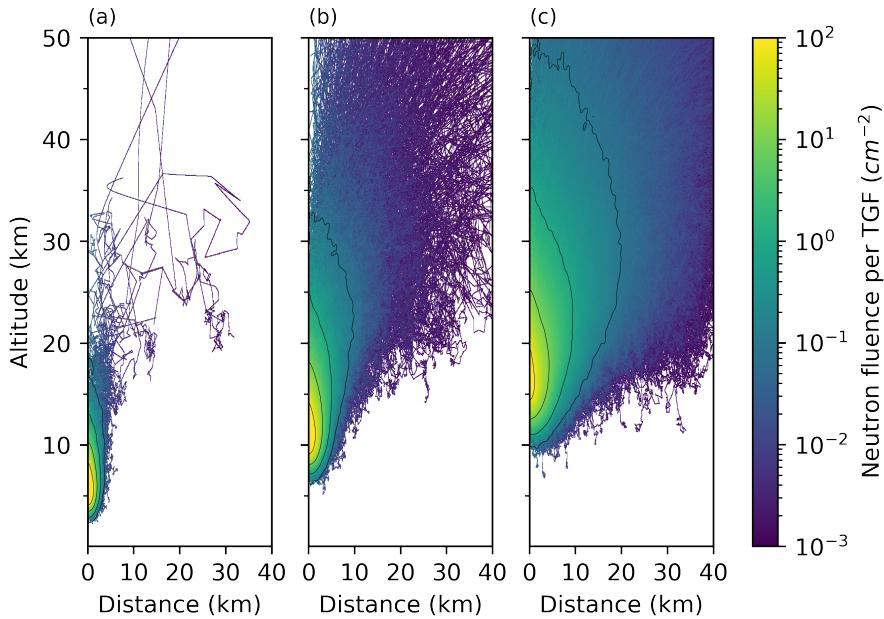
Figure 5. Fluence of neutrons caused by a TGF at an altitude of A) 5 km, B) 10 km, C) 15 km. The depicted isobars show neutron fluences of 10^{-1}, 10^0, 10^1, 10^2 cm^{-2}.

4   Discussion

The MCNP6 calculations reveal the distribution of fluences of various particles caused by vertical TGFs and their energy spectra at different altitudes and radial distances from the TGF axis. The calculations focus mainly on TGF characteristics at altitudes of 0–50 km, where only a few measurements have been performed so far. Such measurements could provide valuable additional information about TGFs and address the limitations of satellite–based observations. However, there are several significant challenges remaining, including delivering detectors to these high altitudes above thunderstorms and designing detectors to maximize the amount of information obtained.

4.1   Means of transportation

The obvious option is to use airplanes, which are easily maneuverable, can stay airborne for a long period, and can reach relatively high altitudes of 12–13 km. Since the top of the thunderstorm cumulonimbus clouds in tropical regions are around 18 km, this might not always be sufficient to fly above the thunderstorm. However, it could be adequate for temperate and polar regions where the tops of the clouds are at altitudes of 13 km and 8 km, respectively (Oceanic and Administration, 2023). Another possibility for using aircraft is during winter thunderstorms, when thunderstorms typically reach altitudes of only several kilometers in temperate regions (Popová et al., 2023; Kolmašová et al., 2022). The advantage of winter thunderstorms is also the possibility to perform various mutual radiation measurements on the ground (Wada et al., 2019; Enoto et al., 2017).
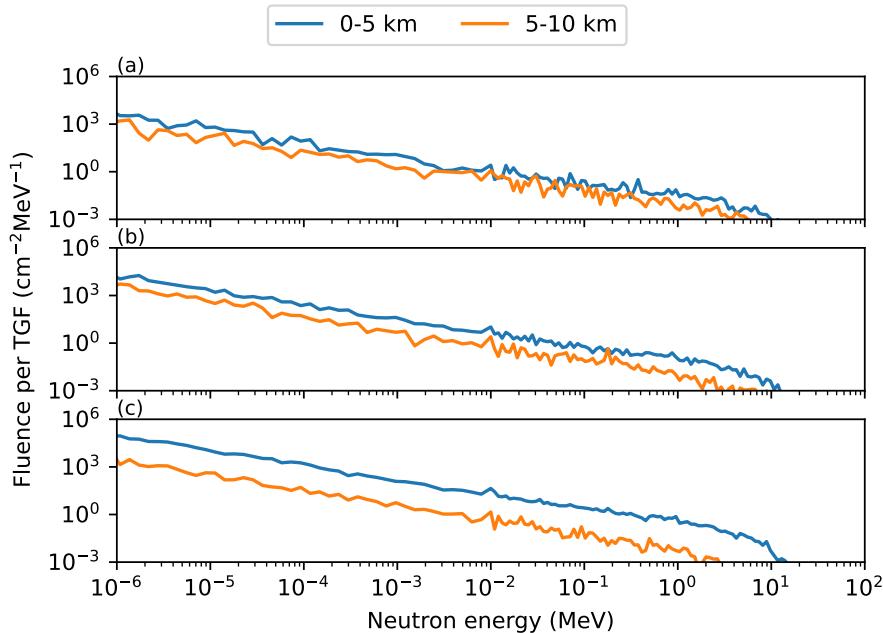
Figure 6. Energy spectra of neutrons caused by a TGF for different radial distances from the TGF origin. The altitude of the TGF origin is 10 km, and the energy spectra are recovered from altitudes of A) 25 km, B) 20 km, C) 15 km.

The drawback of using aircraft for observing winter thunderstorms is that the detectors need to be located relatively close radially to the axis of the TGF, as shown in Fig. 1, Fig. 3, and Fig. 5. Hence, the TGF might miss the detectors even when the aircraft is in the vicinity of an active thunderstorm. Additionally, there are also radiation risks to the aircraft and crew, which

165   might be significant. To avoid the most severe radiation effects of the TGFs, the plane should always stay out of the reach of the primarily accelerated electrons (Dwyer et al., 2010). The potential of using planes for TGF research was demonstrated by the ALOFT campaign, which measured a large number of TGFs (Ostgaard et al., 2023) when the plane was moving above the thunderstorms. Another option is to use weather balloons as carriers of detectors. Weather balloons are usually filled with helium and can ascend up to 35 km, but they cannot be maneuvered, their payload mass is limited, and their use is usually

170   strictly regulated by law. For these reasons, it would likely be difficult to use weather balloons for tracking TGFs above thunderstorms. Nevertheless, measurements with weather balloons would have the advantage of being able to fly above the cloud tops of even the tallest thunderstorms (summer thunderstorms in temperate and tropical regions). Hence, TGFs could be detected at larger radial distances from the TGF axis than for TGFs originating at lower altitudes as was shown in Fig. 1, Fig. 3, and Fig. 5. When weather balloons are launched, they drift with the wind. Although there are online tools for predicting

175   the weather balloon trajectory, it would be very challenging to time the launch so that it flies over a fast–moving, active thunderstorm cell. This would require in–depth experience and expertise in meteorology, weather forecasting, and weather balloon launching. The last suggested option is the use of high–altitude platform stations (HAPS), which could combine the

advantages of aircraft and weather balloons, as some HAPS concepts offer the capability to ascend to altitudes of 20 km, while also providing maneuverability and a large payload capacity (Gonzalo et al., 2018). The disadvantage of HAPS is that they are
180 not widely available.

4.2 Detectors

It was shown that the fluxes and energies of different particle types vary significantly based on the location of the TGF origin, its brightness, and the measurement location. Other variables influencing the fluxes and particle energies include the energy spectrum of the primary electrons, and the tilt of the TGF. We have only considered TGFs with an upward direction, one
185 energy spectrum, and one brightness. These variables also change, as described above, and therefore, the calculated particle fluxes originating from TGFs should be considered as estimates. Nevertheless, these estimates should be sufficient to define the properties of ionizing radiation detectors for TGF detection.

The most significant component of the TGF is bremsstrahlung, which has the largest reach and is relatively easy to detect with various ionizing radiation detectors. The most commonly used detectors are scintillators for their large volumes and
190 high density. Reasonably expected fluences of gamma rays might reach values from 10 cm^{-2} up to 10,000 cm^{-2} per TGF (Fig. 1), whereas the background fluence of cosmic ray photons is around 30 cm^{-2}s^{-1} at an altitude of 20 km and in central Europe. Since the TGF consists of sub–millisecond pulses during which a large number of particles is created, the TGF signal can exceed the background by several folds. Sometimes, the bursts are so intense that scintillator detectors become saturated (Tran15) as the decay of the signal takes hundreds of nanoseconds. In such cases, it is not possible to distinguish individual
195 gamma rays, and information about gamma ray energy and intensity is either lost or diminished. This can be mitigated by using scintillators with faster signal decay times, lower light yield, decreasing the size of the scintillator, or using shielding of the detection element. In general, such precautions reduce the sensitivity of the detector to gamma rays, enabling it to measure high–intensity TGFs. On the other hand, insensitive detectors would not detect TGFs that are farther away or have different energy spectra. Therefore, a combination of gamma ray detectors with various sensitivities would be an effective approach
200 to ensure that energy and intensity information can be recovered from the measurements. Moreover, the energy spectrum can be estimated by analyzing the response of several detectors with different sensitivities to different energies. Such a TGF detector assembly could be similar to a detector used for spectrometry of pulsed radiation fields generated by high–power lasers (Stránský et al., 2021).

The second particle type of interest is electrons, which are likely to be detected in the presence of stronger gamma radiation
205 fields. Reasonably expected fluences of electrons from TGFs are up to 1,000 cm^{-2}, while the background fluence of electrons and positrons is around 2.5 cm^{-2}s^{-1}. For electron detection, a detector with a smaller volume can be used, as electrons directly interact with matter by ionizing it. Therefore, pixel or strip semiconductor detectors or diode–based detectors are suitable because their detection efficiency is much higher than for gamma rays. The advantage of such detectors is that they can be used in a telescopic configuration (multiple diodes), allowing estimation of the incident angle of the electrons if they
210 traverse multiple layers of semiconductor. If the diodes have sufficient volume, the telescope can also function as a calorimeter and provide information about the energy of incident electrons. A limiting factor for semiconductor diodes might be their size,

as scaling diode volume is not straightforward. Therefore, detecting low fluxes of electrons with diodes could be challenging and might require an alternative approach, such as using large–surface scintillators. In a calorimetric configuration, the width of diodes would also be a limiting factor. The energy spectrum of electrons ranges from several keV up to dozens of MeV, which would require several millimeters of semiconductor material to fully stop such energetic electrons. If such detectors are placed on an aircraft, the aircraft skin would likely stop the electrons. Therefore, it might be reasonable to use telescopes in weather balloons instead, since the gondolas of such balloons are typically made of light–weight low–density insulators (e.g., polystyrene) which would not decelerate the electrons significantly. The gondolas can also be designed so that there is a minimum amount of material to shield the electron detectors.

Another component of interest is neutrons. The production of neutrons by photonuclear reactions is inefficient, and the neutron fluxes are relatively low, even in the proximity of the TGF origin (Fig. 5). Moreover, the cross sections of neutron interactions with matter are relatively low, so neutron detectors need to be large to obtain useful information about TGF. This makes them suitable only for platforms that can carry large payloads, such as aircraft. The neutron energies range from meV up to MeV as shown in Fig. 6. Hence, TGF neutron detectors should measure over a very broad range of energies.

4.3 Conclusions

The measurements of TGFs performed directly above the thunderstorms could help overcome the challenges faced by satellites, namely the large attenuation of gamma rays by the atmosphere. Large distances between the TGF origin and detectors onboard satellites cause low statistics of detected gamma rays and blurring of the time structure of TGFs. The measurement campaign with aircraft, weather balloons, or HAPS could provide valuable information about the occurrence of TGFs in various conditions (latitude, lightning, and thunderstorm types) and could resolve the time structure of TGFs with much better accuracy. The findings discussed in previous sections should serve as a study showing the expected fluences, energies, and ranges of ionizing radiation generated by TGFs onboard aircraft and weather balloons. The main findings can be summarized into three points:

1. Estimated fluences of TGF photons measured onboard aircraft or weather balloons could reach up to 10,000 cm^{-2}, and 1,000 cm^{-2} for electrons, for a brightness of 10^{18} primary electrons (>1 MeV). On the other hand, the fluences of neutrons are very low, up to 10 cm^{-2}.

2. TGFs originating at low altitudes have much narrower beams than TGFs originating at higher altitudes. Therefore, the use of weather balloons for the detection of TGFs might be more suitable for high–altitude thunderstorms, such as summer thunderstorms.

3. Features in photon and electron energy spectra, such as maximum energy, ratios between low and high–energy particles, and the presence of 511 keV photons, can be used to estimate the radial distance from the axis of the TGF.

Data availability.

All raw data can be provided by the corresponding authors upon request.

Appendix A

Author contributions.

245   MS, TC performed the Monte Carlo Simulations; MS wrote the manuscript draft; IA, MK, OV, and OP reviewed and edited the manuscript.

Competing interests.

The authors declare that they have no conflict of interest.

Acknowledgements. This work was supported by EU Operational Program Research, Development, and Education in project CRREAT

250   (Research Center of Cosmic Rays and Radiation Events in the Atmosphere) [CZ.02.1.01/0.0/0.0/15_003/0000481].

References

Bowers, G., Smith, D., Kelley, N., Martinez-McKinney, G., Cummer, S., Dwyer, J., Heckman, S., Holzworth, R., Marks, F., Reasor, P., et al.: A terrestrial gamma-ray flash inside the eyewall of hurricane Patricia, Journal of Geophysical Research: Atmospheres, 123, 4977–4987, 2018.

255 Briggs, M. S., Fishman, G., Connaughton, V., Bhat, P., Paciesas, W., Preece, R., Wilson-Hodge, C., Chaplin, V., Kippen, R., Von Kienlin, A., et al.: First results on terrestrial gamma ray flashes from the Fermi Gamma-ray Burst Monitor, Journal of Geophysical Research: Space Physics, 115, 2010.

Celestin, S. and Pasko, V. P.: Energy and fluxes of thermal runaway electrons produced by exponential growth of streamers during the stepping of lightning leaders and in transient luminous events, Journal of Geophysical Research: Space Physics, 116, 2011.

260 Celestin, S., Xu, W., and Pasko, V. P.: Variability in fluence and spectrum of high-energy photon bursts produced by lightning leaders, Journal of Geophysical Research: Space Physics, 120, 10–712, 2015.

Cummer, S. A., Lu, G., Briggs, M. S., Connaughton, V., Xiong, S., Fishman, G. J., and Dwyer, J. R.: The lightning-TGF relationship on microsecond timescales, Geophysical Research Letters, 38, 2011.

Cummer, S. A., Lyu, F., Briggs, M. S., Fitzpatrick, G., Roberts, O. J., and Dwyer, J. R.: Lightning leader altitude progression in terrestrial
265 gamma-ray flashes, Geophysical Research Letters, 42, 7792–7798, 2015.

Dwyer, J., Smith, D., Uman, M., Saleh, Z., Grefenstette, B., Hazelton, B., and Rassoul, H.: Estimation of the fluence of high-energy electron bursts produced by thunderclouds and the resulting radiation doses received in aircraft, Journal of Geophysical Research: Atmospheres, 115, 2010.

Dwyer, J. R.: Source mechanisms of terrestrial gamma-ray flashes, Journal of Geophysical Research: Atmospheres, 113, 2008.

270 Dwyer, J. R. and Smith, D. M.: A comparison between Monte Carlo simulations of runaway breakdown and terrestrial gamma-ray flash observations, Geophysical Research Letters, 32, 2005.

Enoto, T., Wada, Y., Furuta, Y., Nakazawa, K., Yuasa, T., Okuda, K., Makishima, K., Sato, M., Sato, Y., Nakano, T., et al.: Photonuclear reactions triggered by lightning discharge, Nature, 551, 481–484, 2017.

Fishman, G. J., Bhat, P., Mallozzi, R., Horack, J., Koshut, T., Kouveliotou, C., Pendleton, G., Meegan, C., Wilson, R., Paciesas, W., et al.:
275 Discovery of intense gamma-ray flashes of atmospheric origin, Science, 264, 1313–1316, 1994.

Gjesteland, T., Østgaard, N., Laviola, S., Miglietta, M., Arnone, E., Marisaldi, M., Fuschino, F., Collier, A. B., Fabró, F., and Montanya, J.: Observation of intrinsically bright terrestrial gamma ray flashes from the Mediterranean basin, Journal of Geophysical Research: Atmospheres, 120, 12–143, 2015.

Gonzalo, J., López, D., Domínguez, D., García, A., and Escapa, A.: On the capabilities and limitations of high altitude pseudo-satellites,
280 Progress in Aerospace Sciences, 98, 37–56, 2018.

Goorley, J. T., James, M. R., Booth, T. E., Brown, F. B., Bull, J. S., Cox, L. J., Durkee Jr, J. W., Elson, J. S., Fensin, M. L., Forster III, R. A., et al.: Initial MCNP6 release overview-MCNP6 version 1.0, Tech. rep., Los Alamos National Lab.(LANL), Los Alamos, NM (United States), 2013.

Grefenstette, B. W., Smith, D. M., Hazelton, B., and Lopez, L.: First RHESSI terrestrial gamma ray flash catalog, Journal of Geophysical
285 Research: Space Physics, 114, 2009.

Hansen, R., Østgaard, N., Gjesteland, T., and Carlson, B.: How simulated fluence of photons from terrestrial gamma ray flashes at aircraft and balloon altitudes depends on initial parameters, Journal of Geophysical Research: Space Physics, 118, 2333–2339, 2013.

Helmerich, C., McKinney, T., Cavanaugh, E., and Dangelo, S.: TGFs, gamma-ray glows, and direct lightning strike radiation observed during a single flight of a balloon-borne gamma-ray spectrometer, Earth and Space Science, 11, e2023EA003 317, 2024.

290 Kolmašová, I., Santolík, O., Šlegl, J., Popová, J., Sokol, Z., Zacharov, P., Ploc, O., Diendorfer, G., Langer, R., Lán, R., et al.: Continental thunderstorm ground enhancement observed at an exceptionally low altitude, Atmospheric Chemistry and Physics, 22, 7959–7973, 2022.

Lyu, F., Zhang, Y., Lu, G., Zhu, B., Zhang, H., Xu, W., Xiong, S., and Lyu, W.: Recent observations and research progresses of terrestrial gamma-ray flashes during thunderstorms, Science China Earth Sciences, 66, 435–455, 2023.

Maia, J., da Silva, R. C., and Mingacho, J.: Evaluation of effective dose for gamma-rays of terrestrial gamma-ray flashes in aviation: spectral-

295 and atmosphere-effects, Radiation Physics and Chemistry, 215, 111 332, 2024.

Maiorana, C., Marisaldi, M., Lindanger, A., Østgaard, N., Ursi, A., Sarria, D., Galli, M., Labanti, C., Tavani, M., Pittori, C., et al.: The 3rd AGILE terrestrial gamma-ray flashes catalog. Part II: Optimized selection criteria and characteristics of the new sample, Journal of Geophysical Research: Atmospheres, 125, e2019JD031 986, 2020.

Maiorana, C., Marisaldi, M., Füllekrug, M., Soula, S., Lapierre, J., Mezentsev, A., Skeie, C., Heumesser, M., Chanrion, O., Østgaard, N.,

300 et al.: Observation of terrestrial gamma-ray flashes at mid latitude, Journal of Geophysical Research: Atmospheres, 126, e2020JD034 432, 2021.

Marisaldi, M., Fuschino, F., Labanti, C., Galli, M., Longo, F., Del Monte, E., Barbiellini, G., Tavani, M., Giuliani, A., Moretti, E., et al.: Detection of terrestrial gamma ray flashes up to 40 MeV by the AGILE satellite, Journal of Geophysical Research: Space Physics, 115, 2010.

305 Marisaldi, M., Fuschino, F., Tavani, M., Dietrich, S., Price, C., Galli, M., Pittori, C., Verrecchia, F., Mereghetti, S., Cattaneo, P., et al.: Properties of terrestrial gamma ray flashes detected by AGILE MCAL below 30 MeV, Journal of Geophysical Research: Space Physics, 119, 1337–1355, 2014.

Marisaldi, M., Galli, M., Labanti, C., Østgaard, N., Sarria, D., Cummer, S., Lyu, F., Lindanger, A., Campana, R., Ursi, A., et al.: On the high-energy spectral component and fine time structure of terrestrial gamma ray flashes, Journal of Geophysical Research: Atmospheres,

310 124, 7484–7497, 2019.

Neubert, T., Østgaard, N., Reglero, V., Blanc, E., Chanrion, O., Oxborrow, C. A., Orr, A., Tacconi, M., Hartnack, O., and Bhanderi, D. D.: The ASIM mission on the international space station, Space Science Reviews, 215, 1–17, 2019.

Oceanic, N. and Administration, A.: The Four Core Types of Clouds, https://www.noaa.gov/jetstream/clouds/four-core-types-of-clouds, 2023.

315 Østgaard, N., Cummer, S. A., Mezentsev, A., Luque, A., Dwyer, J., Neubert, T., Reglero, V., Marisaldi, M., Kochkin, P., Sarria, D., et al.: Simultaneous observations of EIP, TGF, Elve, and optical lightning, Journal of Geophysical Research: Atmospheres, 126, e2020JD033 921, 2021.

Ostgaard, N., Marisaldi, M., and Lang, T.: Airborne lightning observatory for fegs and tgfs (aloft), 2023.

Pallu, M., Celestin, S., Trompier, F., and Klerlein, M.: Estimation of radiation doses delivered by terrestrial gamma ray flashes within leader-

320 based production models, Journal of Geophysical Research: Atmospheres, 126, e2020JD033 907, 2021.

Petrov, N.: Synchrotron mechanism of X-ray and gamma-ray emissions in lightning and spark discharges, Scientific Reports, 11, 19 824, 2021.

Popová, J., Sokol, Z., Wang, P., and Svoboda, J.: Observations and modelling of the winter thunderstorm on 4 February 2022 at the Milešovka meteorological observatory, Quarterly Journal of the Royal Meteorological Society, 149, 3541–3561, 2023.

325 Roberts, O., Fitzpatrick, G., Stanbro, M., McBreen, S., Briggs, M., Holzworth, R., Grove, J., Chekhtman, A., Cramer, E., and Mailyan, B.: The first Fermi-GBM terrestrial gamma ray flash catalog, Journal of Geophysical Research: Space Physics, 123, 4381–4401, 2018.

Smith, D., Dwyer, J., Hazelton, B., Grefenstette, B., Martinez-McKinney, G., Zhang, Z., Lowell, A., Kelley, N., Splitt, M., Lazarus, S., et al.: A terrestrial gamma ray flash observed from an aircraft, Journal of Geophysical Research: Atmospheres, 116, 2011.

Stadnichuk, E., Svechnikova, E., Nozik, A., Zemlianskaya, D., Khamitov, T., Zelenyy, M., and Dolgonosov, M.: Relativistic runaway electron
330   avalanches within complex thunderstorm electric field structures, Journal of Geophysical Research: Atmospheres, 126, e2021JD035 278, 2021.

Stadnichuk, E., Zemlianskaya, D., Svechnikova, E., Kim, E., Sedelnikov, A., and Anuaruly, O.: Simple reactor model of relativistic runaway electron avalanche development, arXiv preprint arXiv:2301.00542, 2023.

Stránský, V., Istokskaia, V., Versaci, R., Giuffrida, L., Cimmino, A., Margarone, D., and Olšovcová, V.: Development, optimization, and
335   calibration of an active electromagnetic calorimeter for pulsed radiation spectrometry, Journal of Instrumentation, 16, P08 060, 2021.

Tavani, M., Marisaldi, M., Labanti, C., Fuschino, F., Argan, A., Trois, A., Giommi, P., Colafrancesco, S., Pittori, C., Palma, F., et al.: Terrestrial gamma-ray flashes as powerful particle accelerators, Physical review letters, 106, 018 501, 2011.

Tavani, M., Argan, A., Paccagnella, A., Pesoli, A., Palma, F., Gerardin, S., Bagatin, M., Trois, A., Picozza, P., Benvenuti, P., et al.: Possible effects on avionics induced by terrestrial gamma-ray flashes, Natural Hazards and Earth System Sciences, 13, 1127–1133, 2013.

340 Tran, M., Rakov, V., Mallick, S., Dwyer, J., Nag, A., and Heckman, S.: A terrestrial gamma-ray flash recorded at the Lightning Observatory in Gainesville, Florida, Journal of Atmospheric and Solar-Terrestrial Physics, 136, 86–93, 2015.

Ursi, A., Rodriguez Fernandez, G., Tiberia, A., Virgilli, E., Arnone, E., Preziosi, E., Campana, R., and Tavani, M.: A study on tgf detectability at 2165 m altitude: Estimates for the mountain-based gamma-flash experiment, Remote Sensing, 14, 3103, 2022.

Wada, Y., Enoto, T., Nakazawa, K., Furuta, Y., Yuasa, T., Nakamura, Y., Morimoto, T., Matsumoto, T., Makishima, K., and Tsuchiya, H.:
345   Downward terrestrial gamma-ray flash observed in a winter thunderstorm, Physical Review Letters, 123, 061 103, 2019.

Zelenyi, M., Nozik, A., and Stadnichuk, E.: Reactor like TGE model, in: AIP Conference Proceedings, vol. 2163, AIP Publishing, 2019.